Chemistry of Metals and Alloys

Chem. Met. Alloys 8 (2015) 123-128
Ivan Franko National University of Lviv
www.chemetal-journal.org

Quaternary phases $R_{1-x}Ae_xT_2Ge_2$ (R = La, Ce, Gd, Yb; Ae = Ca, Sr; T = Fe, Co, Ni) with $CeAl_2Ga_2$ (122) structure type

Volodymyr GVOZDETSKYI[1,2]*, Viktor HLUKHYY[2], Roman GLADYSHEVSKII[1]

[1] *Department of Inorganic Chemistry, Ivan Franko National University of Lviv, Kyryla i Mefodiya St. 6, 79005 Lviv, Ukraine*
[2] *Department of Inorganic Chemistry, Technical University of Munich, Lichtenbergstr. 4, 85747 Garching, Germany*
* *Corresponding author. Tel.: +380-32-2394506; e-mail: volodymyr.gvozdetskyi@gmail.com*

Received December 8, 2015; accepted December 30, 2015; available on-line September 19, 2016

New quaternary phases crystallizing with the $CeAl_2Ga_2$ (*I*4/*mmm*) structure type (122 phases) were synthesized by arc melting in the *R*–*Ae*-*T*–Ge (*R* = La, Ce, Gd, Yb; *Ae* = Ca, Sr; *T* = Fe, Co, Ni) systems. The structures of $La_{0.590}Ca_{0.410}Fe_2Ge_2$ (a = 4.0662(6), c = 10.625(2) Å) and $La_{0.805}Sr_{0.195}Fe_2Ge_2$ (a = 4.1101(2), c = 10.654(1) Å) were refined on X-ray single-crystal diffraction data. Several new 122 phases were identified on X-ray powder diffraction data in the {Ce,Gd,Yb}-Ca-{Fe,Co,Ni}-Ge systems. The structures are built up from layers of rare-earth or alkaline-earth atoms, alternating with deformed [TGe_4] tetrahedra with tetahedral angles in the range 110° < α < 122° (compared to the ideal value of 109.5°). The influence of the *d*-metal and the *Ae* content on the degree of deformation of the tetrahedra is discussed.

Multicomponent phases / Crystal structure / $CeAl_2Ga_2$ type / X-ray powder and single-crystal diffraction

Introduction

Compounds crystallizing with the $CeAl_2Ga_2$ structure type (Pearson symbol *tI*10, space group *I*4/*mmm*) and known as the 122-type family of superconductive pnictides [1] are intensively investigated at present. Several substituted compounds with this structure type exhibit superconductive transitions at relatively high temperatures. For example, at atmospheric pressure the pure $CaFe_2As_2$ phase is antiferromagnetic below 170 K, but the $Ca_{1-x}Pr_xFe_2As_2$ solid solution ($0.107 < x < 0.127$) shows superconductivity below $T_c \approx 49$ K [2]. Under an applied pressure of 0.69 GPa the $CaFe_2As_2$ compound also becomes superconducting, but with a lower transition temperature, $T_c \approx 10$ K [3]. Representatives of related families are also multicomponent compounds doped with electrons or holes: *e.g.* $LaFeAsO_{1-x}F_x$ (CuZrSiAs structure type, *P*4/*nmm*, $T_c \approx 26$ K, type 1111) [4], $LiFe_{1-x}As$ (PbClF, *P*4/*nmm*, $T_c \approx 18$ K, type 111) [5], $Ca_{1-x}La_xFeAs_2$ (own structure type, *P*2, $T_c \approx 45$ K, type 112) [6], $FeSe_{1-x}$ (PbO, *P*4/*nmm*, $T_c \approx 13$ K, type 11) [7].

Over 600 compounds with 122-type structures are known in different *R*/*Ae*–*T*–*M* (*R* = rare-earth metal, *Ae* = alkaline-earth metal, *T* = transition metal, *M* = main-group element) systems [8], leading to a large number of substitution possibilities. The structures are built up from layers of deformed [TM_4] tetrahedra, which alternate with layers of *R* and *Ae* atoms, and, as shown in [9], the degree of deformation of the tetrahedra has a significant influence on the superconducting transition temperature. Related compounds with this structure type but without toxic arsenic, such as germanides, may also be interesting materials (*e.g.* $BaNi_2Ge_{2-x}P_x$, $SrNi_2Ge_{2-x}P_x$ are superconductors with $T_c \approx 3$ K [10,11]).

In the *Ae*–{Fe,Co,Ni}–Ge systems five compounds with 122-type structure [8,12] are known under normal conditions: $CaCo_2Ge_2$, $CaNi_2Ge_2$, $SrCo_2Ge_2$, $SrNi_2Ge_2$. and $BaCo_2Ge_2$. The $BaNi_2Ge_2$ compound has an orthorhombic structure (own structure type, *oP*20, *Pnma*, a = 8.4693, b = 11.3503, c = 4.3212 Å) at ambient conditions, which transforms to a tetragonal one ($CeAl_2Ga_2$ type) above 753 K [13]. Isostructural $AeFe_2Ge_2$ compounds have not been observed so far. In the *R*–{Fe,Co,Ni}–Ge systems, only $EuFe_2Ge_2$ and $LuFe_2Ge_2$ are missing in the list of known compounds with 122-type structure [8]. The aim of this paper was to carry out $R_{1-x}Ae_x$ substitutions on Fe-, Co-, and Ni-based 122 germanides and investigate the influence on the structural parameters.

Experimental details

Starting materials for the synthesis were ingots of strontium (98 %), calcium (99.5 %), lanthanum (99.9 %), cerium (99.5 %), gadolinium (99.5 %), ytterbium (99.5 %), iron (99.985 %), cobalt (99.95 %), nickel (99.97 %), and germanium (99.999 %). Quaternary alloys with a mass of 0.5 g were synthesized in an arc furnace equipped with a water-cooled copper hearth, using a tungsten electrode under argon atmosphere. The obtained pellets were re-melted three times in order to ensure homogeneity.

The alloys were homogenized in evacuated silica tubes at 673 K for 672 h in a Vulcan A-550 furnace with an automatic temperature control of ±1-2 K. The annealed alloys were quenched in cold water without breaking the ampoules. A special heat treatment procedure was performed for the alloys $La_{1-x}\{Ca,Sr\}_xFe_2Ge_2$, in order to grow single crystals suitable for diffraction studies. The alloys were enclosed in evacuated silica tubes, which were placed in a resistance furnace (Nabertherm P330). The samples were first heated to 1370 K over 6 h and held at that temperature for 2 h. Then, the temperature was lowered at a rate of 0.1 K h^{-1} to 1070 K and maintained for 96 h. The samples were finally cooled to room temperature by switching off the furnace. Well-shaped single crystals were selected for further examination.

Single-crystal intensity data were collected on a STOE IPDS II-T image plate diffractometer (graphite monochromator, Mo $K\alpha$ radiation, λ = 0.71073 Å). A numerical absorption correction was applied [14,15]. Final refinements of the structures were performed with anisotropic displacement parameters for all the atoms (SHELXL-97 [16]). The single crystals investigated on the diffractometer were analyzed with a Jeol SEM 5900LV scanning electron microscope.

X-ray phase and structural analyses were performed using diffraction data obtained on DRON-4.07 (Fe $K\alpha$ radiation, λ = 1.93609 Å) and STOE Stadi P (Cu $K\alpha_1$ radiation, λ = 1.54051 Å) powder diffractometers. For the indexation of the experimental diffraction patterns, theoretical patterns were calculated using the WinXPOW program package [17]. Crystal structure refinements by the Rietveld method were performed using the FullProf program [18].

Results and discussion

Compounds of composition $CaFe_2Ge_2$ and $SrFe_2Ge_2$ do not form at ambient pressure, but the $LaFe_2Ge_2$ compound crystallizes with a $CeAl_2Ga_2$-type structure (a = 4.1059, c = 10.562 Å) [19]. The La atoms can be partially replaced by alkaline-earth atoms (Ca/Sr), retaining the tetragonal 122-type structure. Experimental details and crystallographic data of the two new quaternary phases, refined as $La_{0.590(7)}Ca_{0.410(7)}Fe_2Ge_2$ (a = 4.0662(6), c = 10.625(2) Å) and $La_{0.805(2)}Sr_{0.195(2)}Fe_2Ge_2$ (a = 4.1101(2), c = 10.654(1) Å), are compiled in Tables 1 and 2. The nominal compositions of the alloys, the compositions from the refinements on single-crystal data, and the compositions from EDX analyses, are in good agreement. The same is true for the cell parameters refined on powder and single-crystal data.

Table 1 Experimental details (single-crystal data) and crystallographic data for $La_{0.590(7)}Ca_{0.410(7)}Fe_2Ge_2$ and $La_{0.805(2)}Sr_{0.195(2)}Fe_2Ge_2$ phases (cell parameters refined from powder data are given in square brackets).

Empirical formula		$La_{0.590(7)}Ca_{0.410(7)}Fe_2Ge_2$	$La_{0.805(2)}Sr_{0.195(2)}Fe_2Ge_2$
EDX		La12(2)Ca8(1)Fe40(6)Ge40(9)	La17(4)Sr3(1)Fe42(7)Ge38(9)
Molar mass M_r		356.26	385.53
Space group, Z		*I*4/*mmm*, 2	*I*4/*mmm*, 2
Cell parameters:	a, Å	4.0662(6) [4.0708(1)]	4.1101(2) [4.1151(2)]
	c, Å	10.625(2) [10.6270(4)]	10.654(1) [10.6371(2)]
	V, Å^3	175.67(5) [176.10(2)]	179.98(3) [180.13(2)]
Absorption coefficient μ, mm^{-1}		32.443	36.337
Range of θ, °		3.84-29.99	3.82-32.44
Range of h, k, l		±5, ±5, ±14	±6, ±6, ±16
F(000)		338	316
Crystal size, mm		0.06 × 0.06 × 0.03	0.08 × 0.06 × 0.04
Measured reflections		1854	1926
Independent reflections		102 (R_{int} = 0.095)	125 (R_{int} = 0.040)
Reflections with $F > 2\sigma(F)$		78 (R_σ = 0.032)	105 (R_σ = 0.020)
Number of parameters		10	10
Goof for F^2		1.199	1.193
Final R-indices [$F > 2\sigma(F)$]		$R1$ = 0.037, $wR2$ = 0.031	$R1$ = 0.026, $wR2$ = 0.047
R-indices (all data)		$R1$ = 0.022, $wR2$ = 0.028	$R1$ = 0.021, $wR2$ = 0.046
Residual electron density, e/Å^3		0.67 / -1.42	3.38 / -3.81

The distances between the Fe atoms in the *ab* plane, and between the Ge atoms along the *c* direction, in the $La_{0.590}Ca_{0.410}Fe_2Ge_2$ phase (d_{Fe-Fe} = 2.8752(3), d_{Ge-Ge} = 2.686(1) Å) are shorter than the corresponding distances in the ternary $LaFe_2Ge_2$ compound (d_{Fe-Fe} = 2.903 Å, d_{Ge-Ge} = 2.706 Å). On the contrary, in the $La_{0.805}Sr_{0.195}Fe_2Ge_2$ phase the corresponding interatomic distances (d_{Fe-Fe} = 2.9063(1), d_{Ge-Ge} = 2.741(2) Å) are slightly longer (Fig. 1). The structures of the quaternary phases are built up from less deformed [$FeGe_4$] tetrahedra than the ternary phase.

Table 2 Atomic coordinates and displacement parameters for $La_{0.590(7)}Ca_{0.410(7)}Fe_2Ge_2$ and $La_{0.805(2)}Sr_{0.195(2)}Fe_2Ge_2$.

$La_{0.590(7)}Ca_{0.410(7)}Fe_2Ge_2$ ($CeAl_2Ga_2$, *tI*10, *I*4/*mmm*, *a* = 4.0662(6), *c* = 10.625(2) Å)						
Atom	Wyckoff position	Occupancy	*x*	*y*	*z*	$U_{eq} \times 10^2$, Å^2
La/Ca	2*a*	0.590(7)/0.410(7)	0	0	0	0.65(3)
Fe	4*d*	1	0	½	¼	0.78(3)
Ge	4*e*	1	0	0	0.37361(8)	0.78(3)
$La_{0.805(2)}Sr_{0.195(2)}Fe_2Ge_2$ ($CeAl_2Ga_2$, *tI*10, *I*4/*mmm*, *a* = 4.1101(2), *c* = 10.654(1) Å)						
Atom	Wyckoff position	Occupancy	*x*	*y*	*z*	$U_{eq} \times 10^2$, Å^2
La/Sr	2*a*	0.805(2)/0.195(2)	0	0	0	0.97(3)
Fe	4*d*	1	0	½	¼	1.08(4)
Ge	4*e*	1	0	0	0.37136(11)	1.00(3)

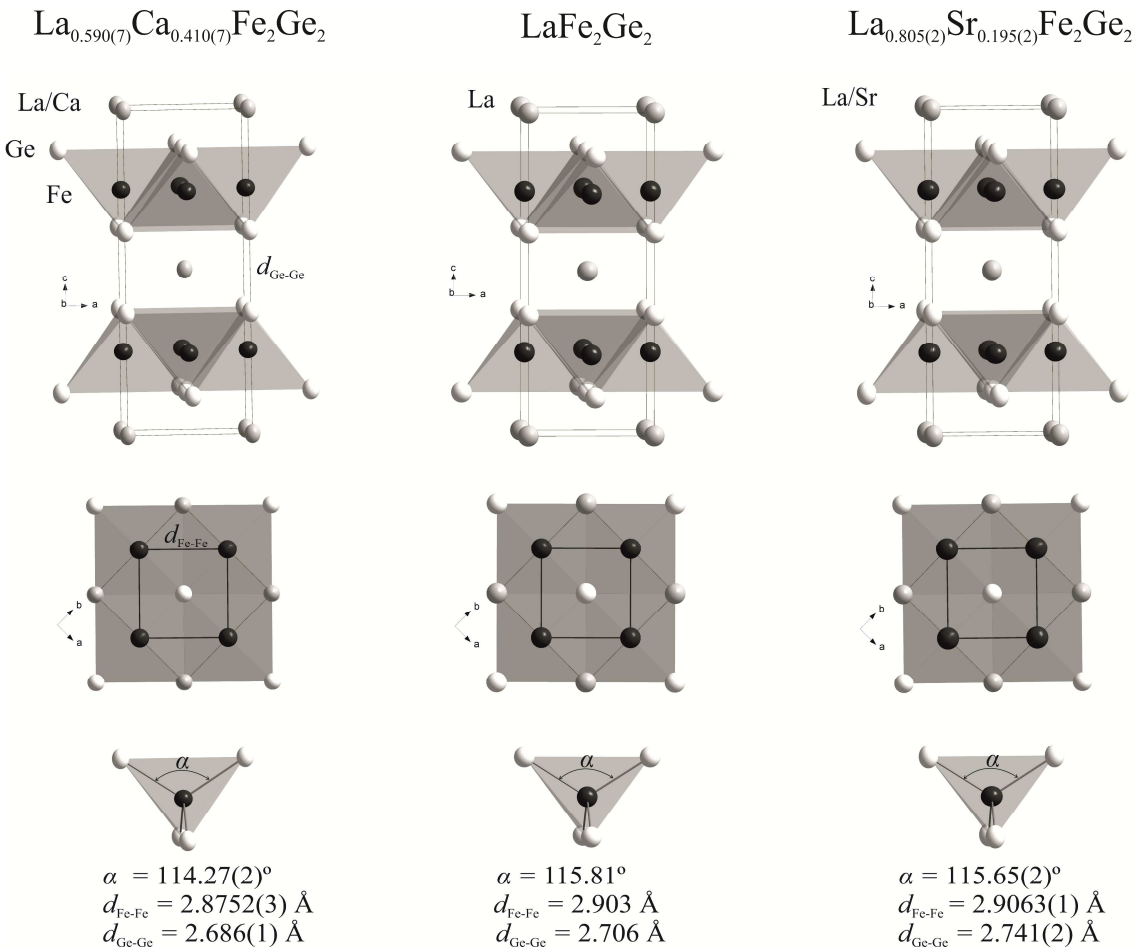

Fig. 1 Crystal structures of the quaternary 122 phases $La_{0.590(7)}Ca_{0.410(7)}Fe_2Ge_2$ and $La_{0.805(2)}Sr_{0.195(2)}Fe_2Ge_2$, comparing with the ternary compound $LaFe_2Ge_2$.

Several new isostructural phases were synthesized in the {Ce,Gd,Yb}–Ca–{Fe,Co,Ni}–Ge quaternary systems (preliminary data in [20]). The crystal structure refinements showed the formation of solid solutions with the composition ranges and cell parameters listed in Table 3. The values of the unit-cell parameters of these phases are comparable to those of the isotypic compounds in the corresponding ternary systems: $CeFe_2Ge_2$ (a = 4.0713, c = 10.483 Å) [21,22], $CeCo_2Ge_2$ (a = 4.071, c = 10.170 Å) [21], $CeNi_2Ge_2$ (a = 4.150, c = 9.854 Å) [21], $GdFe_2Ge_2$ (a = 3.9867, c = 10.4798 Å) [21,23], $GdCo_2Ge_2$ (a = 3.996, c = 10.066 Å) [21], $GdNi_2Ge_2$ (a = 4.063, c = 9.783 Å) [21], $YbFe_2Ge_2$ (a = 3.924, c = 10.503 Å) [24], $YbCo_2Ge_2$ (a = 3.9311, c = 10.040 Å) [25], $YbNi_2Ge_2$ (a = 4.001, c = 9.733 Å) [21], $CaCo_2Ge_2$ (a = 3.99, c = 10.298 Å) [19], and $CaNi_2Ge_2$ (a = 4.0749, c = 9.987 Å) [19]. Within each solid solution, the c-parameter of the tetragonal $CeAl_2Ga_2$-type phase increases with increasing Ca content (Fig. 2). The a-parameter decreases with increasing Ca content when R = Ce, increases when R = Yb, and remains nearly the same when R = Gd. The replacement Fe→Co→Ni decreases the c-parameter and increases the a-parameter. As noted earlier, the main motifs of these structures are layers containing edge-sharing [TGe$_4$] tetrahedra, parallel to the ab plane and separated by R/Ae atoms. It can be seen from Table 3 that the cell dimensions of the new 122-phases cover a wide range of values. These can be related to the deviation of the central angle of the [TGe$_4$] tetrahedra from the ideal value of 109.5°, shown in the last column of the table. In the structures of the phases studied here, this angle, α = Ge-T-Ge, varies within the range 110° < α < 122°. Taking into consideration the fact that superconductive behavior in similar compounds (several types of iron-based superconductors have been identified in the recent years, the most prominent being the 1111, 122, 111, and the 11 families mentioned above) has been related to the value of α, the new 122-phases offer a possibility to tune the superconductive properties. The Co-based phases are built up of less deformed [TGe$_4$] tetrahedra, compared to the Fe- or Ni-based phases.

The choice of the d-metal (Fe, Co or Ni) has a significant influence on the structural parameters of the 122 phases. This arises from the increasing number of electrons in the d-orbitals in the row Fe→Co→Ni. The additional electrons provided by Co [$3d^7 4s^2$] and Ni [$3d^8 4s^2$] with respect to Fe [$3d^6 4s^2$] would have to occupy anti-bonding bands [26-28], and therefore the interatomic distances between d-metal atoms must increase, as can be seen in Fig. 2 (the shortest distances between T atoms are proportional to the a-parameter of the unit cell, $d_{T\text{-}T} = a/\sqrt{2}$). The [$TGe_4$] tetrahedra exhibit broadening in the ab plane, which is accompanied by compression along the c-direction and, therefore, decrease of the c-parameter. As a consequence, the degree of deformation of the tetrahedra increases in the row α[FeGe$_4$] < α[CoGe$_4$] < α[NiGe$_4$]. Substitution of Ca for La in the ternary $LaFe_2Ge_2$ compound results in reduced electron concentration in the $R_{1-x}Ae_x$ layers (Ca [$4s^2$] compared with La [$5d^1 6s^2$]), which will also influence the bonding in the [TGe$_4$] tetrahedra. In agreement with the reasoning made above, the [FeGe$_4$] tetrahedra in $La_{0.590}Ca_{0.410}Fe_2Ge_2$ (α = 114.27°) are less deformed than those in $LaFe_2Ge_2$ (α = 115.81°), the difference being ~1.5°. A similar effect is expected in the case of the Sr-substituted phase $La_{0.805}Sr_{0.195}Fe_2Ge_2$ (α = 115.65°). Here, however, the considerably larger Sr atoms (size factor) have an opposite influence on the structure, and the result is a limited decrease of ~0.15° for the α-angle. Within the row Ce [$4f^1 5d^1 6s^2$] → Gd [$4f^7 5d^1 6s^2$] → Yb [$4f^{14} 5d^0 6s^2$] the valence electron concentration decreases. Therefore, the strongest electron effect (which causes a reduction of the α-angle in the [TGe$_4$] tetrahedra) due to the substitution of Ca for R atoms is observed for the Ce-containing phases (see Fig. 2). The decrease of the tetrahedral α-angle in the structures of the Gd-containing phases is less sharp than for the Ce-containing ones. When R = Yb, no decrease of the electron concentration is achieved, but, over against due to increasing ionic interaction between the [$Yb_{1-x}Ca_x$] and [TGe$_4$] layers, the electron concentration in the tetrahedra may slightly increase, which would explain that the [TGe$_4$] tetrahedra in the

Table 3 Solid solutions with $CeAl_2Ga_2$-type structure in the quaternary systems {Ce,Gd,Yb}–Ca–{Fe,Co,Ni}–Ge: composition range, cell parameters and tetrahedral angle (α).

System	x	a, Å	c, Å	α, °
$Ce_{1-x}Ca_xFe_2Ge_2$	0.116(7)-0.797(9)	4.06666(9)-4.0063(2)	10.5034(3)-10.6553(7)	113.76(5)-111.7(1)
$Ce_{1-x}Ca_xCo_2Ge_2$	0.18(1)-0.792(9)	4.06009(9)-4.0066(2)	10.2009(3)-10.2930(7)	118.64(4)-115.1(1)
$Ce_{1-x}Ca_xNi_2Ge_2$	0.099(5)-0.882(6)	4.14955(8)-4.0870(1)	9.8606(2)-9.9777(5)	121.47(4)-118.88(9)
$Gd_{1-x}Ca_xFe_2Ge_2$	0.043(5)-0.472(6)	3.98615(7)-3.9877(1)	10.4934(2)-10.5675(3)	112.78(4)-111.94(4)
$Gd_{1-x}Ca_xCo_2Ge_2$	0.075(8)-0.900(4)	3.99269(5)-3.9879(1)	10.0913(2)-10.2952(4)	116.52(4)-116.19(7)
$Gd_{1-x}Ca_xNi_2Ge_2$	0.106(4)-0.837(4)	4.06737(7)-4.0795(2)	9.8122(2)-9.9597(5)	119.62(4)-119.0(1)
$Yb_{1-x}Ca_xFe_2Ge_2$	0.246(7)-0.696(2)	3.94199(8)-3.97196(9)	10.5428(3)-10.6436(3)	110.48(5)-111.40(4)
$Yb_{1-x}Ca_xCo_2Ge_2$	0.31(1)-0.755(4)	3.9492(5)-3.9821(2)	10.1112(7)-10.2439(6)	114.34(8)-115.68(8)
$Yb_{1-x}Ca_xNi_2Ge_2$	0.281(3)-0.755(1)	4.02544(7)-4.06357(7)	9.8411(3)-9.9537(2)	118.22(4)-118.4(1)

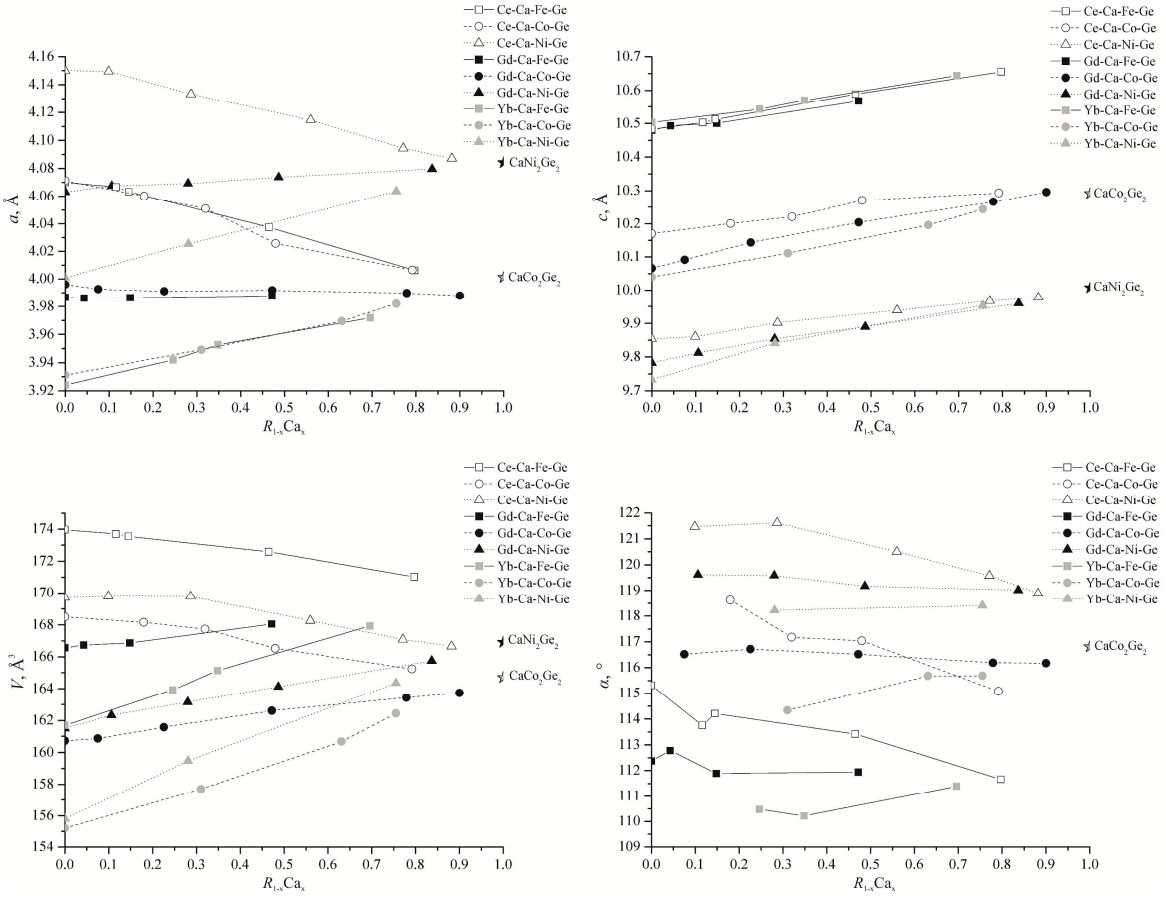

Fig. 2 Cell parameters and *α*-angles inside the [*T*Ge$_4$] tetrahedra in the structures of the phases with CeAl$_2$Ga$_2$-type structures in the quaternary systems {Ce,Gd,Yb}–Ca–{Fe,Co,Ni}–Ge.

Yb$_{1-x}$Ca$_x$*T*$_2$Ge$_2$ phases become more deformed with increasing Ca content. The significance of the electronic factor has been confirmed by the replacement of four-valent Ge by five-valent Sb in the 122-homologues EuNi$_{2-x}$Sb$_2$ and SrNi$_{2-x}$Sb$_2$ [27,29]. The substitution leads to an unusual increase of the electron concentration in the [NiSb$_4$] tetrahedra, which is compensated by Ni defects.

Conclusions

Ae–*T*–*Pn* (*Ae* = alkaline-earth element; *T* = transition metal; *Pn* = pnictogen) systems are intensively investigated because of the existence of superconductors with 122 composition and CeAl$_2$Ga$_2$-type structure. These phases may show superconductive transitions at relatively high temperatures, which can be related to the value of the *α*-angle, *i.e.* the *Pn*-*T*-*Pn* angle at the center of the [*TPn*$_4$] tetrahedra. The new homologue phases $R_{1-x}Ae_xT_2Ge_2$ (*R* = La, Ce, Gd, Yb; *Ae* = Ca, Sr, *T* = Fe, Co, Ni) cover a wide range of values of the tetrahedral angle (110° < *α* < 122°), depending on the type of *d*-metal and the *R*/*Ae* content. The value of the *α*-angle increases within the row *α*[FeGe$_4$] < *α*[CoGe$_4$] < *α*[NiGe$_4$], because of the increase of the number of electrons in anti-bonding bands. Similarly, substitution of Ca atoms for the *R* atoms decreases the *α*-angle when the number of valence electrons in the $4f^n5d^m6s^2$ configuration is larger than for the Ca atoms (for *R* = La, Ce, Gd). There is no difference in the case where *R* = Yb [$4f^{14}5d^06s^2$] and the slightly larger deformation observed with increasing Ca content may here be due to ionic interactions between the [Yb$_{1-x}$Ca$_x$] atoms and the [*T*Ge$_4$] tetrahedra .

Acknowledgements

This work was supported by the Ministry of Education and Sciences of Ukraine under the grant No. 0115U003257, and by the Deutscher Akademischer Auslandsdienst for a research stipend (V.G.) at the Technical University of Munich (grant No. A/12/85156).

References

[1] K. Ishida, Y. Nakai, H. Hosono, *J. Phys. Soc. Jpn.* 78/6 (2009) 062001 (20 p).

[2] B. Lv, L. Deng, M. Gooch, F. Wei, Y. Sun, J.K. Meen, Y. Xue, B. Lorenz, C. Chu, *Proc. Natl. Acad. Sci. U.S.A.* 108/38 (2011) 15705-15709.

[3] T. Park, E. Park, H. Lee, T. Klimczuk, E.D. Bauer, F. Ronning, J.D. Thompson, *J. Phys.: Condens. Matter* 20 (2008) 322204 (3 p).

[4] Y. Kamihara, T. Watanabe, M. Hirano, H. Hosono, *J. Am. Chem. Soc.* 130 (2008) 3296-3297.

[5] X.C. Wang, Q.Q. Liu, Y.X. Lv, W.B. Gao, L.X. Yang, R.C. Yu, F.Y. Li, C.Q. Jin, *Solid State Commun.* 148 (2008) 538-540.

[6] N. Katayama, K. Kudo, S. Onari, T. Mizukami, K. Sugawara, Y. Sugiyama, Y. Kitahama, K. Iba, K. Fujimura, N. Nishimoto, M. Nohara, H. Sawa, *J. Phys. Soc. Jpn.* 82 (2013) 123702 (4 p).

[7] S. Margadonna, Y. Takabayashi, M.T. McDonald, K. Kasperkiewic, Y. Mizuguchi,Y. Takano, A.N. Fitch, E. Suard, K. Prassides, *Chem. Commun.* 43 (2008) 5607-5609.

[8] P. Villars, K. Cenzual (Eds.), *Pearson's Crystal Data. Crystal Structure Database for Inorganic Compounds*, Release 2013/14, ASM International, Materials Park (OH), 2013.

[9] ZA.. Ren, G.C. Che, X.L. Dong, J. Yang, W. Lu, W. Yi, X.L. Shen, Z.C. Li, L.L. Sun, F. Zhou and Z.X. Zhao, *EPL* 83 (2008) 17002 (4 p).

[10] D. Hirai, F. von Rohr, R.J. Cava, *Phys. Rev. B* 86 (2012) 100505(R) (5 p).

[11] V. Hlukhyy, A.V. Hoffmann, V. Grinenko, J. Scheiter, F. Hummel, D. Johrendt, T.F. Fässler, *Phys. Status Solidi B: Basic Solid State Phys.* (submitted).

[12] L. Siggelkow, V. Hlukhyy, T.F. Fässler, *Z. Anorg. Allg. Chem.* 636 (2010) 378.

[13] V. Hlukhyy, A. Hoffmann, T.F. Fässler, *Z. Anorg. Allg. Chem.* 638 (2012) 1619.

[14] *X-RED* (1.26), *Data Reduction Program*, STOE & Cie, Darmstadt, Germany, 2004.

[15] *X-SHAPE* (2.05), *Crystal Optimization for Numerical Absorption Correction*, STOE & Cie, Darmstadt, Germany, 2004.

[16] G.M. Sheldrick, *Acta Crystallogr. A* 64 (2008) 112-122.

[17] *STOE WinXPow* 3.0.2.1, STOE & Cie GmbH, Darmstadt, Germany, 2011.

[18] J. Rodriguez-Carvajal, *IUCr Newsletter.* 26 (2001) 12-29.

[19] G. Venturini, B. Malaman, *J. Alloys Compd.* 235 (1996) 201-209.

[20] V. Gvozdetskyi, R. Gladyshevskii, *Coll. Abstr. XII Int. Conf. Cryst. Chem. Intermet. Compd.*, Lviv, 2013, p. 191.

[21] W. Rieger, E. Parthé, *Monatsh. Chem.* 100 (1969) 444-454.

[22] V. Gvozdetskyi, N. German, R. Gladyshevskii, *Visn. Lviv. Univ. Ser. Khim.* 54 (2013) 11-18.

[23] V. Gvozdetskyi, N. German, R. Gladyshevskii, *Visn. Lviv. Univ. Ser. Khim.* 53 (2012) 12-19.

[24] D. Rossi, R. Marazza, R. Ferro, *J. Less-Common Met.* 58 (1978) 203-207.

[25] O.L. Sologub, P.S. Salamakha, G. Bocelli, S. Otani, T. Takabatake, *J. Alloys Compd.* 312 (2000) 196-200.

[26] W. Jeitschko, M. Reehuis, *J. Phys. Chem. Solids.* 48/7 (1987) 667-673.

[27] W.K. Hofmann, W. Jeitschko, *J. Less-Common Met.* 138 (1988) 313-322.

[28] C. Zheng, R. Hoffmann, *J. Solid State Chem.* 72 (1988) 58-71.

[29] V. Gvozdetskyi, V. Hlukhyy, T.F. Fässler, R. Gladyshevskii, *Z. Anorg. Allg. Chem.* 641/11 (2015) 1859-1862.